Carpathian Journal of Earth and Environmental Sciences, February 2022, Vol. 17, No. 1, p. 131 – 142; DOI:10.26471/cjees/2022/017/207

STRUCTURAL CONTROLS ON DRAINAGE PATTERN USING INTEGRATION OF REMOTE SENSING AND STRUCTURAL DATA: INSIGHTS FROM CAIRO-SUEZ PROVINCE, EGYPT

Ahmed HENAISH[1], Sherif KHARBISH[2*] & Sara ZAMZAM[1]

[1]Department of Geology, Faculty of Science, Zagazig University, 44519, Egypt; email: ahmed_henaish@yahoo.com
*[2]Department of Geology, Faculty of Science, Suez University, Suez Governorate, El Salam City, 43518, Egypt; email: sherif.kharbish@suezuni.edu.eg, *corresponding author*

Abstract: The Cairo-Suez Province (CSP) is one of the highly deformed settings in northern Egypt that includes a complex structures and drainage network. The scope of this paper is to present the results of investigation as how far can geological structures control and/or affect the distribution of drainage networks based on insights from several selected sites along CSP. High resolution satellite images are used with field extracted structural data in order to clarify the structural setting of the studies areas. Moreover, hill shaded digital elevation maps (DEMs) are set up for the studied sites in order to compare the structural features with the resulted structural maps. Additionally, GIS based tools are used for extracting drainage network from DEMs. Trend analysis is used for comparing the drainage network to the main resulted structural elements. As a result, nine different structural models are suggested to control the drainage pattern along CSP. These models are placed under main three structural categories which are; simple fault(s), linked faults and fault-related folds. Additionally, the resulted structural models show main controls on sedimentation as well as groundwater accumulation. The findings of the research are helpful as preliminary step for groundwater studies, sedimentation, and geo-hazard assessment.

Keywords: Structural control, Remote sensing, Drainage pattern, Cairo-Suez Province, Sedimentation, Geographic information system (GIS)

1. INTRODUCTION

The identification and analysis of drainage network witness great and wide interest in many studies and researches. This interest is due to the positive and negative impacts of drainage system on the environment in various regions. Additionally, drainage network analysis is considered one of the important and major factors in studies concerned with groundwater accumulation and flow (e.g., Hunt et al., 2015; Jesiya & Gopinath, 2020; Ahmed et al, 2021; Mseli et al., 2021; Ndhlovu & Woyessa, 2021), environmental hazards assessment including flash floods (e.g., Alam et al., 2020; Prama et al., 2020; Hassan et al., 2021; Kruczkiewicz et al., 2021) and initiation of faults and their development by growth tectonic processes (e.g., Giaconia et al., 2013). Moreover, drainage network and streams are considered the most important factors of erosion, transportation and deposition of sediments; in which the eroded materials resulted from surface water flow are accumulated within the flood plain of a stream (Athmer & Luthi, 2011; Earle, 2019).

Drainage patterns and streams have been defined into different basic types, such as trellis, dendritic, rectangular, parallel, radial, contorted and annular (Howard, 1967). These diverse types are due to the sensitivity of drainage patterns in their nature by many conditions such as regional slope, rock hardness, lithological types, climate and tectonic setting (e.g., Strahler, 1964; Earle, 2019). The most powerful of these conditions on the pattern of drainage tributaries is the structure features within the rock beneath (Deffontaines et al., 1997; Ali & Ali, 2018). As it is considered that any deflection from dendritic type (other drainage pattern types) are controlled by structures and lithological variations (Pubellier et al., 1994).

Relationship between geologic structures and drainage pattern is intimate and has been discussed in

many publications (e.g., Macka, 2003; Delcaillau et al., 2006; Odeh et al., 2016; Wołosiewicz, 2018). Additionally, flow direction can be controlled by many structural features including; faults, fractures, fold axes and dipping sedimentary strata. Therefore, while analyzing the development of a drainage network, it is usually supposed that the network progressively regulates its path to the underlying geologic structure during its extension into the accessible space. Geological structures exert a significant control on drainage development, especially, in active basins, for example, the control of relay ramps on drainage pattern and sedimentation (e.g., Moustafa & Khalil, 2017).

Recently, remote sensing data of various spectral and spatial resolution is being used effectively in drainage pattern delineation, water flow, terrain analysis and structural features mapping with utilizing multi spatial analysis tools of Geographic Information Systems (GIS) (e.g., Tlapáková et al., 2015; Singh et al., 2019; Attwa & Zamzam, 2020; Khalifa et al., 2021; Jothimani et al., 2021).

The main objectives of this research are to throw light on the relationship between different types and geometries of faults and folds to drainage patterns from many insights along the CSP, Egypt (Fig. 1). Additionally, the effect of drainage pattern on sedimentation is discussed at specific areas comprising syn- and post-rift sediments. In this manner, six areas have been selected from CSP, representing the major structure geometries including faults and fault-related folds. The present study based on geological field mapping integrated to high resolution satellite images and the analysis of digital elevation models using GIS tools. The results of the present study can suggest critical data for managing surface and groundwater resources. Also, the results could be helpful in identifying potential groundwater zones, flood risk analysis, and selecting suitable sites for building water harvesting structures.

2. REGIONAL GEOLOGICAL AND GEOMORPHOLOGIC FRAMEWORK

Geologically, the CSP (Fig. 1) possess the northern part of the Egyptian Eastern Desert and comprises a part of the unstable shelf. It extends for about 120 km from Cairo city at the west to Suez

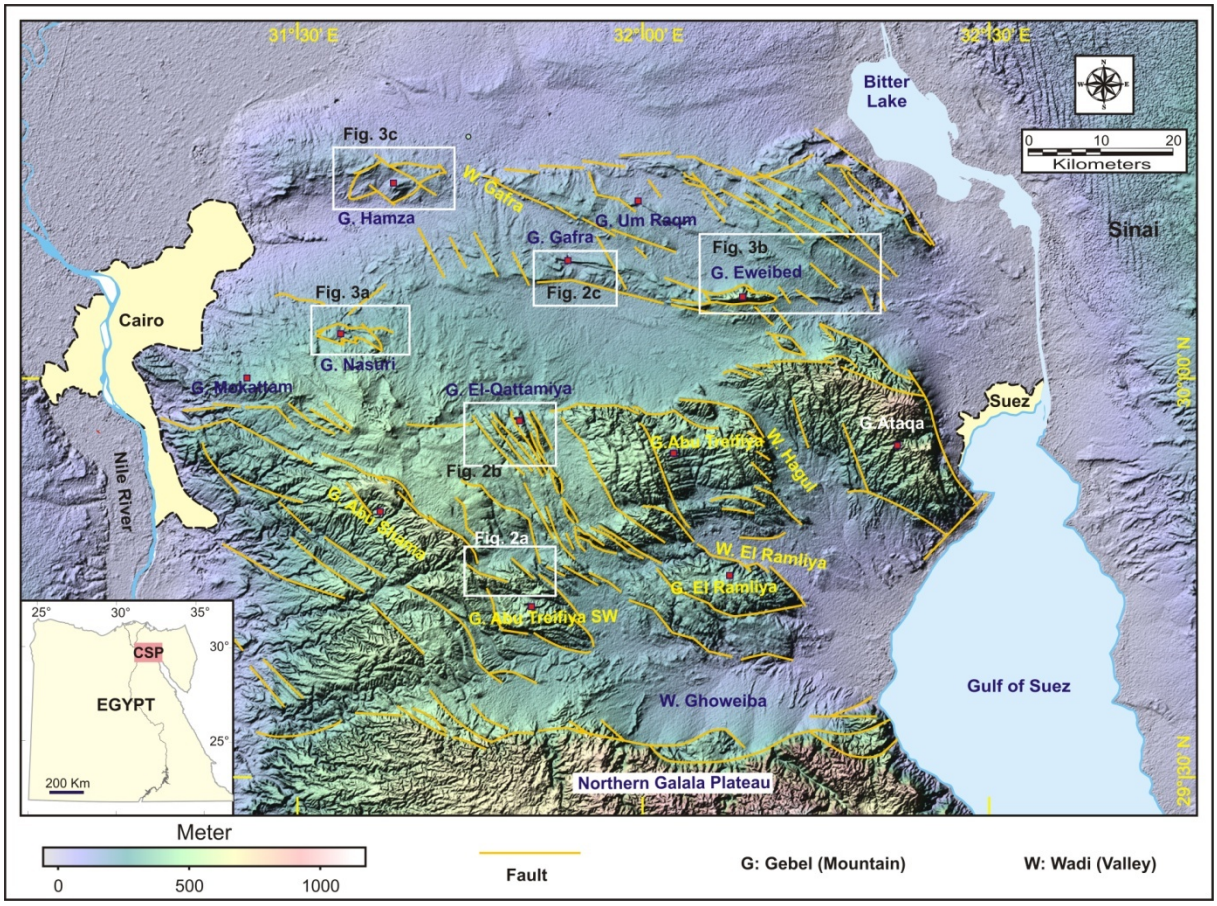

Figure 1. Shaded relief map (SRTM DEM) with some geological elements: major faults and structural blocks along CSP (compiled from Moustafa & Abd-Allah 1992; Attwa & Henaish, 2018; Henaish & Kharbish, 2020). Note, G: Gebel (mountain).

city at the east. Tectonically, The CSP experienced several deformation events encountered with the movements involving Arabian, African and Eurasian plates. These tectonic events include; (1) Jurassic-Early Cretaceous rifting phase, (2) Late Creataceous transpressive movement and (3) Late Oligocene-Early Miocene extension related to the Gulf of Suez opening and sustained to the post-Miocene period. As a result, such tectonic episodes affect the distribution of rock units along CSP which comprises Cretaceous, Eocene, Oligocene, Miocene, Pliocene and Quaternary sediments.

From structural geology point of view, the CSP can be divided into two main sectors which are represented by a number of uplifted blocks and down-faulted sub-basins. The northern province is characterized by faulting as well as folding affecting Cretaceous, Eocene, Oligocene and Miocene outcrops (e.g. G. Eweibed; G. Gafra; G. Shabraweet; G. Umm Raqm; G. Hamza; G. Um Qamar), (Fig. 1). In contrast, the southern province is represented by several distinguished Eocene fault blocks and less folded sequences (e.g. G. Ataqa; G. Nasuri; Qattamiya; G. Abu Shama; G. Abu Treifiya SW), (Fig. 1). Additionally, the CSP is a prominent district of E-W extended fault belts of left-stepped en echelon normal faults (e.g. Moustafa et al., 1998) and NW-SE trending normal faults. These fault belts were formed by dextral transtension due to throw transfer on faults from the Gulf of Suez to the CSP (Moustafa & Abd-Allah, 1992). Furthermore, they enclose different normal fault geometries and linkage styles (e.g. Henaish & Attwa, 2018; Henaish & Kharbish, 2020; Kharbish et al., 2020), (Fig. 1).

Geomorphologically, the CSP extends from east of the Nile fluvial plain to west of Suez Canal and the northern part of Gulf of Suez (Fig. 1). Generally, the elevation profile of the CSP is gradually decreased toward the north. The high elevation and steep slopes have been observed in the south part of the CSP (Fig. 1) at which the altitude reach to 850 m above mean sea level such as G. Ataqa at the eastern side of the CSP. On the other hand, land in the northern part is mainly flat with 70% of its landmass up to ~ 150 m above mean sea level except some localized hilly scarps such as G. Eweibed (~ 400 m) and G. Gafra (~ 200 m) (Fig. 1). The regional slope ranges from 0° to 68° and the average annual precipitation for the study area is 70 mm/y.

In general, the dissected high elevated mountains at the southern part are separated by a definite drainage pattern and interfluves, while the northern part is characterized by widespread patterns (dendritic) due to its flat and gently dipping topographic surface. Wadi Gafra (Fig. 1) is the most distinguished one in the northern region with dendritic network for its master stream and their branches. It is characterized by a dense network of tributaries that extend more in width based on slope and permeability of rocks. In the southern CSP, Wadi Ghoweiba, Wadi Hagul and Wadi El Ramliya (Fig. 1) are the large extended ones. Obviously, the main wadies are structurally controlled, where they extend along major faults, while tributaries are related to lithologically, fracturing and/or regional slope.

3. STRUCTURAL SETTING

Structural mapping seeks to characterize rock deformation that registered brittle or ductile deformation. This in turn can affect the geomorphology and hence, the drainage pattern. Accordingly, structural mapping was achieved in detail at several selected study sites (Figs. 2 and 3). In this research the interpreted geological structures are compiled based on field structural mapping of Henaish (2018a, b), Attwa & Henaish (2018), Henaish & Kharbish (2020) and Attwa et al., (2020). Additionally, in the present study, new interpreted geological structures and modification were added according to new field data. The attitudes of bedding planes as well as structural elements of each area have been traced on high resolution GoogleEarth images.

Regarding structural elements and their geometrical characteristics, six areas have been chosen from CSP representing drainage pattern related to folds as well as faults, which are; the northern part of G. Abu Treifiya SW, G. Qattamiya, G. Gafra, G. Nasuri, G. Hamza and G. Eweibed (Figs. 2 and 3). Starting with normal fault arrays, the first mapped area is represented G. Abu Treifiya SW (Fig. 2a) which lies at the southern sector of CSP. The outcrop rock units are represented by Middle Eocene as well as Upper Eocene sediments which show low dip angles ranging from 4° to 10°. The northern part of G. Abu Treifiya SW is characterized by several relay ramps which are breached in some locations. Normal fault planes strike toward the NW and NNW directions with steep dip angles (70°-80°).

The G. Qattamiya area is the mapped second site representing structures of normal fault arrays (Fig. 2b). It is represented by Middle Eocene rock units with low dip values that reach 6°. Also, Upper Eocene rock units are exposed at the downthrown sides of normal faults and have dip values that range from 10° to 15°. The Gebel Qattamiya block comprises sets of NNW- with subordinate E-striking normal faults. The overall structure geometry of the block is represented by horst-graben structures. The third mapped sector is represented by inward hard-

linked faults at the southern scarp of G. Gafra (Fig. 2c). It comprises Oligocene and Miocene rock units with gentle dip values. Moreover, Quaternary sediments lie at the downthrown side of the southern border faults forming fan delta. The southern sector of G. Gafra is dissected by WNW- to NW-striking normal faults and a single ENE-trending fault. Also, Oligocene and Miocene rock units are affected by folding related to the nearby faults.

From the study sites, the first areal deformed by fault-related folds is represented by G. Nasuri (Fig. 3a). The main core of G. Nasuri fold comprises Middle Eocene rocks with gentle dipping flanks that have dip angles of 12°-20°. The fold axis is sub-parallel (i.e. acute angle of 2°-30°) to the bounding conjugate faults that strike toward the NW and NE directions. The Nasuri fold is formed as a result of drag along the footwalls of the bounding normal faults (Henaish, 2018a). At the eastern side of G. Nasuri an anticline and synclinal folds lie affecting the Upper Eocene rocks and Oligocene sediments, respectively. Other gentle fault-related folds are lying to the north at the downthrown sides of normal faults affecting the Oligocene sediments.

The eastern CSP comprises a well-known anticline fold with Upper Eocene core which is called G. Eweibed (Fig. 3b). It has an E-W trending fold axis that is sub-parallel to the bounding E-W, NE-SW and NW-SE normal fault segments. To the east of Gebel Eweibed, several NW-striking en echelon normal faults cut the Miocene sediments. Also, two major NW-trending anticlinal folds are formed as a result of drag along the footwalls of the NW-striking normal fault segments with Oligocene fold cores.

At the western side of CSP, Gebel Hamza (Fig. 3c) is representing a major ENE-trending anticlinal drag fold with northern and southern Miocene flanks and Oligocene core. Both fold limbs show gentle dip values of 8°-15°, whereas the Oligocene core is highly eroded. The G. Hamza fold is bounded from all sides by ENE- and NE striking normal faults, also, several NE-SW trending faults are dissecting limbs and the core of the fold. The normal faults have steep dip angles that reach 70°. At the southwestern and northeastern parts of G. Hamza, the intersection of normal faults revealed inward hard-linked faults where Miocene and Quaternary sediments are exposed at the downthrown sides of the intersected faults.

4. REMOTE SENSING DATA

Active remote sensing data (i.e., radar sensor) is the best technology in drainage network mapping as well as geological structures displaying and extraction (e.g., Prabhakar et al., 2019; Raju et al., 2020; Abdelouhed et al., 2021), especially Shuttle Radar Topography Mission Global 1 arc second (SRTMGL1). This data is estimated by the National Aeronautics and Space Administration (NASA) and the National Geospatial-Intelligence Agency (NGA) to obtain near global scale elevation data in order to generate a complete high-resolution digital topographic record of the Earth's surface. In our study area, four SRTMGL1 images with 30 m spatial resolution were downloaded from the US Geological Survey (USGS) website in order to cover all the investigated area. Although there are many

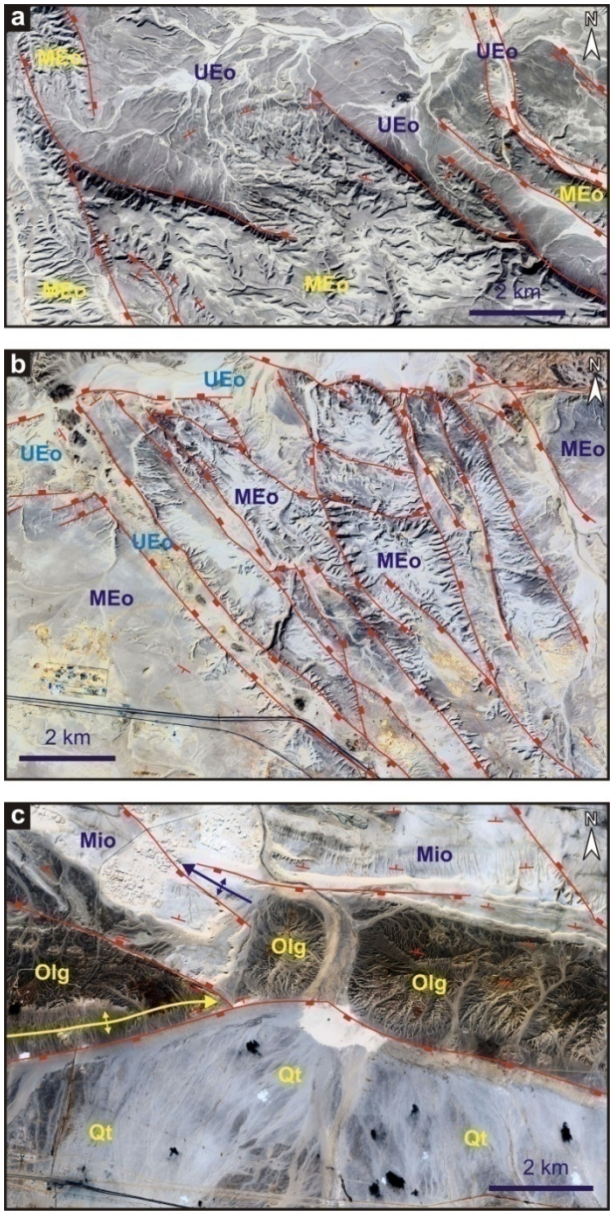

Figure 2. Major structural features (i.e. faults and folds) affecting (a) northern G. Abu Treifiya SW, (b) G. Qattamiya and (c) southern G. Gafra.

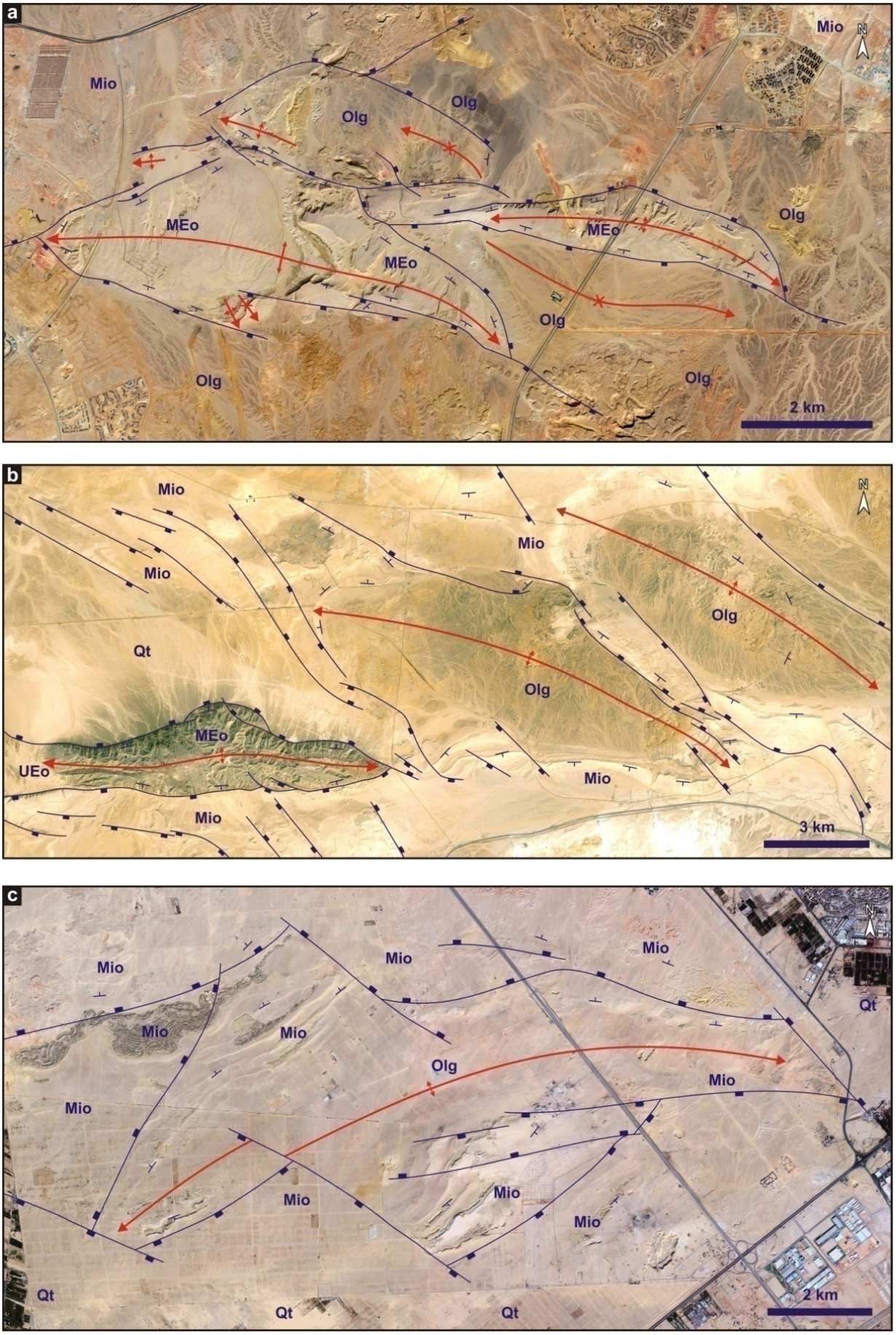

Figure 3. Major structural features (i.e. faults and folds) affecting (a) G. Nasuri, (b) G. Eweibed and (c) G. Hamza.

recent scenes for the investigated areas, the downloaded SRTMGL1 images recorded at February 2000 were utilized in order to avoid the impact of many man-made and urban features that invaded the mapped areas.

Different GIS spatial analysis tools were used to facilitate and achieve the aim of the research. Firstly, the utilized SRTMGL1 images were combined using ArcGIS mosaic to new raster tool and clipped into six images according to the interested regions. Secondly, in order to delineate the drainage pattern, clipped SRTMGL1 images have been analyzed using ArcGIS hydro tools according to the following ordered functions: Fill Sink, flow direction, accumulation, stream definition, segmentation and then using the Drainage Line Processing task to produce the stream network. Moreover, the flow direction image of each region was resembled to show the relationship between the flow path of the stream network with the regional slope and structural features in this region. On the other hand, the clipped images were relief shaded using ArcGIS Hillshade Analyst tool. The image for each region was shaded into two main products with different azimuth angles for enhancing fine linear variations in the surface that consider very useful step in lithological discontinuities mapping (e.g. Smith & Clark, 2005; Abdullah et al., 2010). These shade images were integrated into one image through Weighted Sum tool and then the structure features have been able to be distinguished visually.

5. RESULTS AND DISCUSSION

In the present research, pseudo-colored shaded relief images are helpful in enhancing different linear and curvilinear features for the selected analyze sites that may indicate faults and fold structures as shown in Figures 4 and 5. Moreover, changes in terrain texture and pattern can also help in extracting information about rock types as displayed at southern G. Gafra site (Fig. 4c). Regarding to the extracted drainage pattern; trellis, dendritic and radial patterns are developed along the selected sites. Two different drainage network systems are observed: the old drainage system which includes high order branches (6^{th}, 5^{th} and 4^{th}) and the recent drainage one that includes smaller order branches (Figs. 4 and 5). The oldest drainage network in the study sites is the only 6^{th} order stream that recorded at southern G. Gafra site with a main NW-SE direction (Fig. 4c). In some cases the branches of the drainage pattern and faults present relatively different directions, which indicate that it is affected by regional slope and not, directly, by tectonics. Obviously, the flow direction of the drainage pattern at the study sites is characterized by highly dynamic water flow systems due to the variation in topography, heterogeneity in lithology and structural complexity. These variable flow directions will be explained in the following paragraphs.

By studying and correlating the drainage pattern along CSP, it is observed that they are mainly controlled by different structural geometries that are mainly faults and fault-related folds in addition to dip direction of bedding planes. The correlation between field mapped structures supported by high resolution GoogleEarth images as well as drainage extracted from DEMs revealed nine different models of structural geometries controlling drainage pattern. This comparison based on the analysis of geometry and attitude (in the form of rose diagrams) of mapped structures and the extracted drainage (Figs. 4 and 5). These models are resulted from three main types of geological structures which are; simple fault plane(s), linked faults (soft- or hard-linkage) and extensional folds.

The first type is represented by single normal fault plane (Fig. 6a, b) that causes two different drainage patterns according to the dip direction of bedding planes related to the nearby fault and the resulted cut-off angle between the fault and bedding planes. Where the dip direction of bedding planes is antithetic to the fault plane with an acute cut-off angle, the stream tends to drain parallel to the fault plane; hence, the direction of sediment entry points is parallel to the dip direction of the fault plane. Contrarily, where the dip direction of bedding planes is synthetic to the fault plane, with an obtuse cut-off angle, the drainage is likely to flow perpendicular or oblique to the fault plane, hence, the direction of sediment entry points is in opposition to the dip direction of the fault plane. Additionally, more complex type is represented by normal fault arrays forming simple horst-graben structure (Fig. 6c) as shown in Gebel Qattamiya (Figs. 2b and 4b). In this type drainage can be either parallel or perpendicular to the fault plane according to the dip direction of bedding planes as in the first type, also, sedimentation is favorable at structural lows or grabens (e.g., Trudgill, 2002).

The second type is represented by drainage pattern related to linked normal fault segments. In extensional tectonic settings, normal fault segments grow in length and height where they can interfere. Where the tips of faults are not linked, fault segments can be either overlapped or underlapped, hence, fault segments are described as soft-linked (e.g, Fossen & Rotevatn, 2016; Henaish, 2021). Obstinately, where fault segments linked on map or cross-section scale, they are described as hard-linked (e.g, Savastano et al., 2017).The soft-linked faults (Fig. 6d) are well-

represented at Gebel Abu Treifiya SW by a simple relay ramp formed between two overlapped NW-oriented normal faults (Figs. 2a and 4a). The resulted drainage pattern is found to be related to the dip direction of the relay ramp also it controls the sediment entry point. It is worth mentioning that Moustafa & Khalil (2017) concluded that relay ramps control both drainage pattern and sedimentation based on many examples from the Gulf of Suez and CSP (e.g. G. Ataqa).

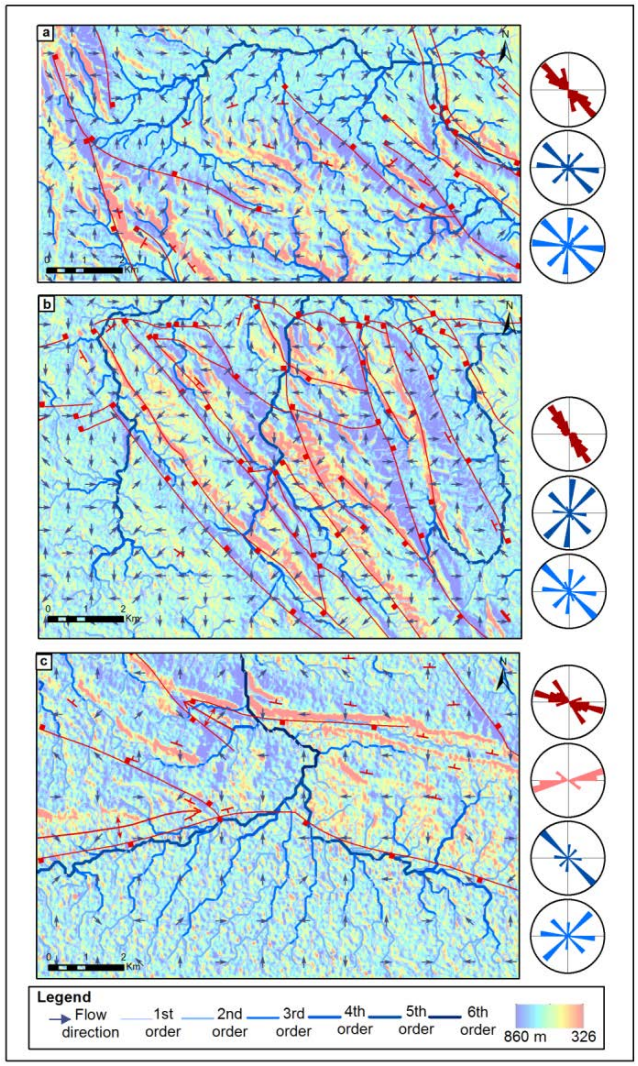

Figure 4. Extracted drainage network with the mapped structures overlaid on hill shaded SRTM DEM image and their trend analysis (Rose diagrams RDs) of (a) northern G. Abu Treifiya SW, (b) G. Qattamiya and (c) southern G. Gafra. (Note, red RD related to faults; pink RD for folds; dark blue RD for main streams (high orders) and bright blue RD for tributaries (low orders).

At the study sites, hard-linked faults can be found at several places. Two examples of large-scale inward hard-linked faults have been compared from at the southwestern part of G. Hamza (Figs. 3c and 5c) and the southern scarp G. Gafra (Figs. 2c and 4c). At G. Hamza, the drainage catchments emerge at the footwall of the linked faults where sedimentation rises at the hanging-wall of linked faults in the form of Miocene rocks and Quaternary sediments (Figs. 5c and 6e). Defiantly, drainage catchments at the southern scarp of G. Gafra emerge at the hanging-wall side of the inward linked faults. In such case, this pattern is resulted from what so called reversed drainage (e.g., Anagnostoudi et al., 2010). This happens as the flow direction of drainage is reversed due to higher topographies resulted from sedimentation of Quaternary sediments at the hanging-wall of the linked faults (Figs. 2c and 6f).

The third type of structural controlled drainage pattern in the present study is represented by fold structures. In the selected study sites, mapping and analysis of folds revealed that they are formed as extensional folds along conjugate fold arrays or as transfer structures between overlapped faults. The results of the extracted drainage related to folded surfaces geometry revealed three models of drainage pattern (Figs. 6g, h, i). The investigation of G. Eweibed area (Figs. 3b and 5b) revealed that drainage pattern is drain away from fold crest (i.e., away from the fold axis) of anticline folds in accordance to the dip direction of folded strata. Also, the nose of plunging folds controls the drainage pattern according to the plunge of fold axis. On the other hand, synclinal folds (Fig. 6h) show that drainage pattern is down streamed towards the fold trough (i.e., towards the fold axis) and then parallel to the fold axis according to the plunge (e.g. east G. Nasuri).

The abovementioned characteristics of drainage pattern related to folded surfaces represents the ideal case. However, folds encountered by faulting, show different drainage pattern. For example, the anticlines of G. Nasuri (Figs. 3a and 5a), which are affected by many faults parallel to the fold axis, show difference in drainage pattern than those of G. Eweibed area (Figs. 3b and 5b). Also, at G. Hamza (Figs. 3c and 5c), it is clear that drainage pattern flow parallel to fold axis rather than the dip direction of folded bedding planes. This is attributed to, the crestal part erosion of the anticline fold of G. Hamza (Fig. 6i). Attwa et al., (2020) concluded that G. Hamza fold shows a topographic low at the core of the fold due to erosion of the fold crest. It is worth mentioning that they mapped many near surface groundwater aquifers at the fold core of G. Hamza anticline where they are controlled by faulting.

6. CONCLUSION

Analyzing drainage network systems represent an initial key step that can be helpful in many issues

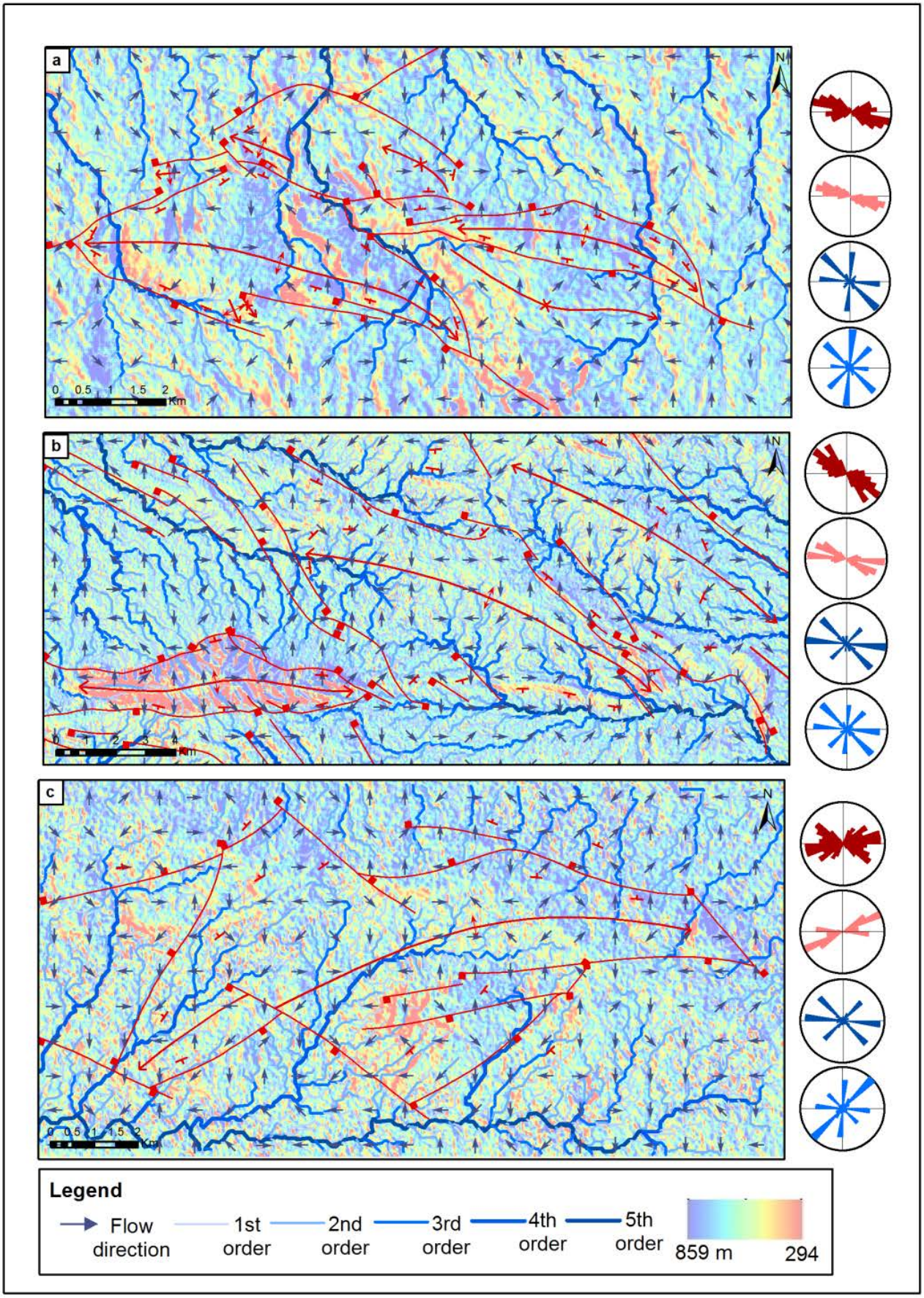

Figure 5. Extracted drainage network with the mapped structures overlaid on hill shaded SRTM DEM image and their trend analysis (Rose diagrams RDs) for (a) G. Nasuri, (b) G. Eweibed and (c) G. Hamza. (Note, red RD related to faults; pink RD for folds; dark blue RD for main streams (high orders) and bright blue RD for tributaries (low orders).

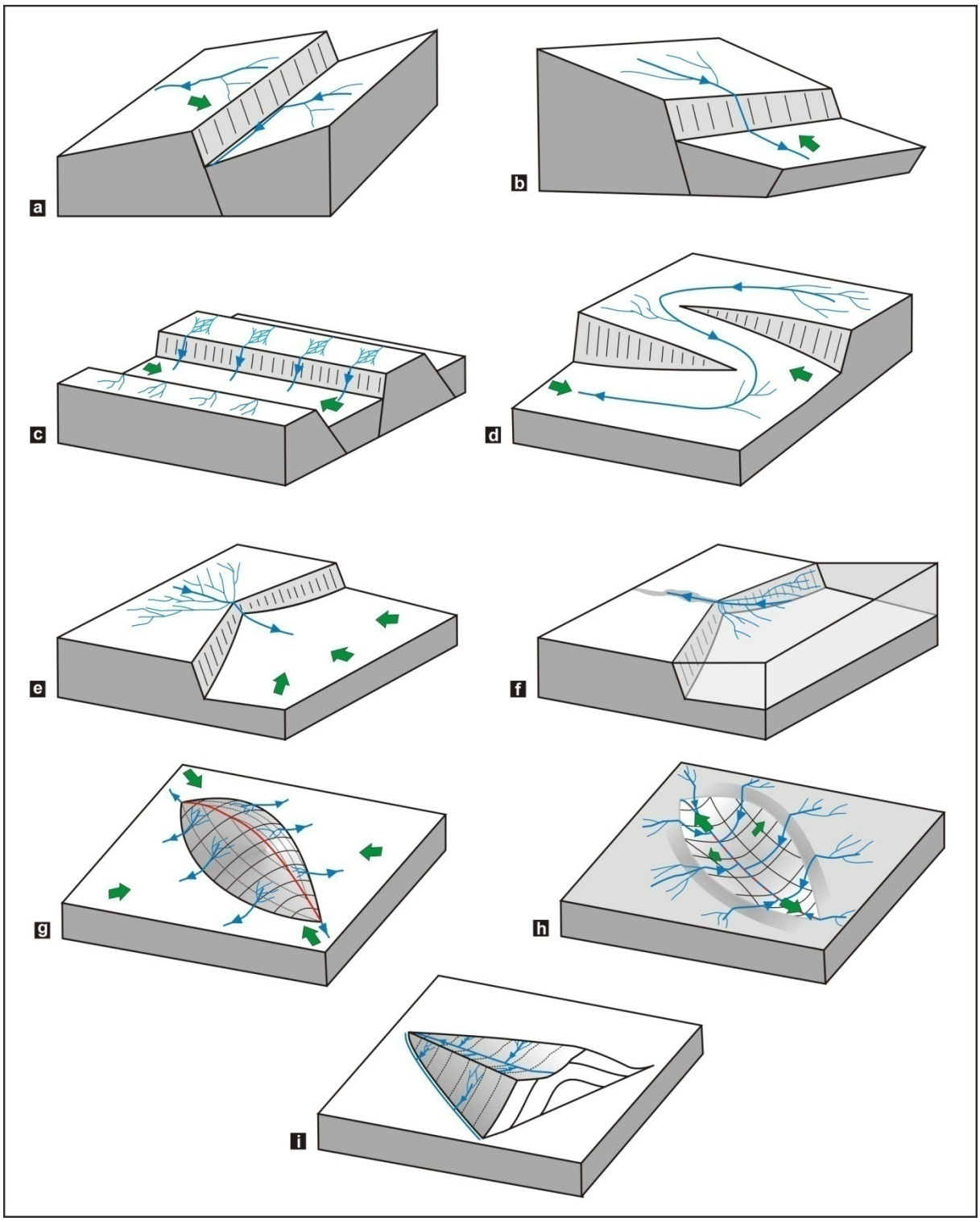

Figure 6. Suggested models of structural-controlled drainage at the present study.

including; groundwater flow, environmental hazards assessment, fault activity and sedimentation. Also, geological structures have major controls on drainage network in active tectonic settings. In this manner, the present study focused on structural controls on drainage pattern using incorporation of structural data and analyzed remote sensing data at CSP. Mapped geological structures based on field data were correlated to hill shaded SRTM DEM images for six selected analyze sites. As result, a concordance was observed between the mapped structures and the linear as well as curvilinear features detected on hill shaded images. Moreover, drainage network system was extracted from SRTM DEM images using GIS based tools.

Trellis, radial and dendritic patterns were the most observed drainage types in the studied sites.

Additionally, by evaluating the results of trend analysis for the main streams and tributaries as well as geological structures; there is a normally relationship between them. Accordingly, nine models of geological structures controlling drainage systems were suggested. These models are mainly related to three main categories including; simple fault plane(s), linked faults and fault-related folds. Also, it was found that these models can control sedimentation and groundwater accumulation along CSP. Such models could be helpful for geo-related studies in highly deformed settings.

Acknowledgement

The authors would like to thank Prof. Mohammed Attwa, Zagazig University (Egypt), for his support through field trips.

REFERENCES

Abdelouhed, F., Ahmed, A., Abdellah, A. & Mohammed, I., 2021. *Lineament mapping in the Iknioun area (Eastern Anti-Atlas, Morocco) using Landsat-8 Oli and SRTM data.* Remote Sensing Applications: Society and Environment, 23, 100606.

Abdullah, A., Akhir, J.M., & Abdullah, I., 2010. *Automatic mapping of lineaments using shaded relief images derived from digital elevation model (DEMs) in the Maran–Sungi Lembing area, Malaysia.* Electronic Journal of Geotechnical Engineering, 15(6), 949-958.

Ahmed, A., Alrajhi, A. & Alquwaizany, A.S., 2021. *Identification of Groundwater Potential Recharge Zones in Flinders Ranges, South Australia Using Remote Sensing, GIS, and MIF Techniques.* Water, 13, 2571, https://doi.org/10.3390/ w13182571.

Alam, A., Ahmed, B. & Sammonds, P., 2020**.** *Flash flood susceptibility assessment using the parameters of drainage basin morphometry in SE Bangladesh.* Quaternary International, DOI: https://doi.org/10.1016/j.quaint.2020.04.047.

Ali, U. & Ali, S.A. 2018. *Investigation of Drainage for Structures, Lithology and Priority (Flood and Landslide) Assessment Using Geospatial Technology, J&K, NW Himalaya.* V. P. Singh et al. (eds.), Hydrologic Modeling, Water Science and Technology Library 81, https://doi.org/10.1007/978-981-10-5801-1_11.

Anagnostoudi, Th., Papadopoulou, S., Ktenas, D., Gkadri, E., Pyliotis, I., Kokkidis, N., & Panagiotopoulos, V., 2010. *The Olvios, Rethis and Inachos drainage system evolution and human activities influnce of their future evolution.* Bulletin of the Geological Society of Greece, 43(2), 548-557.

Athmer, W. & Luthi, S.M., 2011. *The effect of relay ramps on sediment routes and deposition: A review.* Sedimentary Geology, 242, 1-17.

Attwa, M. & Henaish, A. 2018. *Regional structural mapping using a combined geological and geophysical approach - A preliminary study at Cairo-Suez district, Egypt.* Journal of African Earth Sciences, 144, 104-121. DOI: https://doi.org/10.1016/j.jafrearsci.2018.04.010

Attwa, M. & Zamzam, S. 2020. *An integrated approach of GIS and geoelectrical techniques for wastewater leakage investigations: Active constraint balancing and genetic algorithms application.* Journal of Applied Geophysics, 175, 103992. DOI: https://doi.org/10.1016/j.jappgeo.2020.103992

Attwa, M., Henaish, A. & Zamzam, S. 2020. *Hydrogeologic characterization of a fault-related dome Using outcrop, borehole and electrical resistivity data.* Natural Resources Research 29, 1143–1161. DOI: https://doi.org/10.1007/s11053-019-09504-6

Deffontaines, B., Lacombe, O., Angelier, J., Chu, H.T., Mouthereau, F., Lee, C.T., Deramond, J., Lee, J.F., Yu, M.S. & Liew, P.M. 1997. *Quaternary transfer faulting in the Taiwan foothills: evidence from a multisource approach.* Tectonophysics, 274(1), 61–82.

Delcaillau, B., Carozza J.M. & Laville, E., 2006. *Recent fold growth and drainage development: The Janauri and Chandigarh anticlines in the Siwalik foothills, northwest India.* Geomorphology, 76, 241-256.

Earle, S. 2019. *Physical Geology - 2nd Edition*. Victoria, B.C.: BCcampus. Retrieved from https://opentextbc.ca/physicalgeology2ed/.

Fossen, H. & Rotevatn, A. 2016. *Fault linkage and relay structures in extensional settings- A review.* Earth-Science Reviews, 154, 14-28.

Giaconia, F., Guillermo Booth-Rea, G, Martínez-Martínez, J.M., Azañón J.M., Joaquín Pérez-Romero, J. & Villegas, I., 2013. *Mountain front migration and drainage captures related to fault segment linkage and growth: The Polopos transpressive fault zone (southeastern Betics, SE Spain).* Journal of Structural Geology, 46, 76-91.

Hassan, A., Albanai, J.A. & Goudie, A., 2021**.** *Modeling and managing flash flood Hazards in the State of Kuwait.* Preprints2021070011 (https://doi.org/10.20944/preprints202107.0011.v1).

Henaish, A. & Attwa, M., 2018. *Internal structural architecture of a soft-linkage transfer zone using outcrop and DC resistivity data: Implications for preliminary engineering assessment*. Engineering Geology, 244, 1-13. DOI: https://doi.org/10.1016/j.enggeo.2018.07.018

Henaish, A. & Kharbish, S., 2020. *Linkage style of rift-associated fault arrays: insights from central Cairo-Suez district, Egypt.* Carpathian Journal of Earth and Environmental Sciences 15 (1), 189-196. 10.26471/cjees/2020/015/121

Henaish, A., 2018a**.** *Soft-linkage transfer zones: Insights from the Northern Eastern Desert, Egypt*. Marine

and Petroleum Geology, 95, 265-275. DOI: https://doi.org/10.1016/j.marpetgeo.2018.05.005

Henaish, A., 2018b. *Fault-related domes: Insights from sedimentary outcrops at the northern tip of the Gulf of Suez rift, Egypt.* Marine and Petroleum Geology, 91, 202-210. DOI: https://doi.org/10.1016/j.marpetgeo.2018.01.009

Henaish, A., 2021**.** *Structural architecture and tectonic evolution of Haimour block, Gulf of Aqaba, Egypt: An example of multiphase deformed stepover*. Marine and Petroleum Geology, 134, 105332. DOI: https://doi.org/10.1016/j.marpetgeo.2021.105332

Howard, A.D., 1967. *Drainage analysis in geological interpretation: a summation*. Am Asso Petrol Geol Bull, 51(11), 2246–2259.

Hunt, B.B., Smith, B.A., Andrews, A., Wierman, D.A., Broun, A.S., & Gary, M.O., 2015. *Relay ramp structures and their influence on groundwater flow in the Edwards and Trinity Aquifers, Hays and Travis Counties, central Texas***,** in Doctor, D.H., Land, L., and Stephenson J.B., eds., Sinkholes and the Engineering and Environmental Impacts of Karst: Proceedings of the Fourteenth Multidisciplinary Conference, October 5-9, Rochester, Minnesota: NCKRI Symposium 5: Carlsbad, New Mexico, National Cave and Karst Research Institute, 189-200.

Jesiya, N.P. & Gopinath, G., 2020. *A fuzzy based MCDM–GIS framework to evaluate groundwater potential index for sustainable groundwater management - A case study in an urbanperiurban ensemble, southern India.* Groundwater for Sustainable Development, DOI: https:// doi.org/10.1016/j.gsd.2020.100466.

Jothimani, M., Abebeb, A. & Duraisamy, R., 2021. *Drainage Morphometric Analysis of Shope watershed, Rift Valley, Ethiopia: Remote sensing and GIS-based approach.* IOP Conf. Series: Earth and Environmental Science, 796, 012009, doi:10.1088/1755-1315/796/1/012009.

Khalifa, A., Bashir, B., Çakir, Z., Kaya, Ş., Alsalman, A. & Henaish, A., 2021**.** *Paradigm of Geological Mapping of the Adıyaman Fault Zone of Eastern Turkey Using Landsat 8 Remotely Sensed Data Coupled with PCA, ICA, and MNFA Techniques.* ISPRS International Journal of Geo-Information, 10, 368. DOI: https://doi.org/10.3390/ijgi10060368

Kharbish, S., Henaish, A. & Zamzam, S., 2020. *Geodiversity and geotourism in Greater Cairo area, Egypt: implications for geoheritage revival and sustainable development.* Arabian Journal of Geosciences, 13, 451.

Kruczkiewicz, A., Bucherie, A., Ayala, F., Hultquist, C., Vergara, H., Mason, S., Bazo, J. & de Sherbinin, A., 2021. *Development of a Flash Flood Confidence Index from Disaster Reports and Geophysical Susceptibility.* Remote Sens., 13, 2764, https://doi.org/10.3390/rs13142764.

Macka, Z., 2003**.** *Structural control on drainage network orientation an example from the Loucka drainage basin, SE margin of the Bohemian Massif (S Moravia, Czech Rep.).* Landform Analysis, 4, 109-117.

Moustafa, A.R. & Abd-Allah, M.A., 1992**.** *Transfer zones with en echelon faulting at the northern end of the Suez rift*. Tectonics 11, 499-509.

Moustafa, A.R. & Khalil, S., 2017. *Control of extensional transfer zones on syntectonic and posttectonic sedimentation: implications for hydrocarbon exploration.* Journal of the Geological Society (London), 174, 318-335.

Moustafa, A.R., El Badrawy, R. & Gibali, H., 1998. *Pervasive E-ENE oriented faults in northern Egypt and their effect on the development and inversion of prolific sedimentary basins.* In: 14th E.G.P.C. Petrol. Conf. (pp. 51-67). Cairo, Egypt.

Mseli, Z.H., Mwegoha, W.J., & Gaduputi, S., 2021. *Identification of potential groundwater recharge zones at Makutupora basin, Dodoma Tanzania*. Geology, Ecology, and Landscapes, DOI: 10.1080/24749508.2021.1952763.

Ndhlovu, G.Z. & Woyessa, Y.E., 2021. *Integrated Assessment of Groundwater Potential Using Geospatial Techniques in Southern Africa: A Case Study in the Zambezi River Basin.* Water, 13, 2610, https://doi.org/10.3390/w13192610.

Odeh, T., Gloaguen, R., Mohammad, AS.H. & Schirmer, M., 2016. *Structural control on drainage network and catchment area geomorphology in the Dead Sea area: an evaluation using remote sensing and geographic information systems in the Wadi Zerka Ma'in catchment area (Jordan).* Environmental Earth Sciences, 75, 482.

Prabhakar, A.K., Singh, K.K., Lohani, A.K. & Chandniha, S.K., 2019. *Study of Champua watershed for management of resources by usingmorphometric analysis and satellite imagery.* Applied Water Science, 9:127.

Prama, M., Omran, A., Schröder, D. & Abouelmagd, A. 2020. *Vulnerability assessment of flash floods in Wadi Dahab Basin, Egypt.* Environmental Earth Sciences, 79:114, https://doi.org/10.1007/s12665-020-8860-5.

Pubellier, M., Deffontaines, B., Quebral, R. & Rangin, C., 1994. *Drainage network analysis and tectonics of Mindanao, southern Philippines*. Geomorphology, 9(4), 325–342.

Raju, S.R, Raju, S.G. & Rajasekhar M., 2020. *Morphometric analysis of Mandavi River Basin in Rayalaseema region of Andhra Pradesh (South India), using remote sensing and GIS.* Journal Ind.Geophys. Union, 24(1), 54-67.

Savastano, V.L.M., Schmitt, R.S., M´ario Neto Cavalcanti Araújo, M.N.C. & Inocˆencioc, L.C., 2017**.** *Rift brittle deformation of SE-Brazilian continental margin: kinematic analysis of onshore structures relative to the transfer and accommodation zones of southern Campos Basin.* Journal of Structural Geology, 94, 136-153.

Singh, V., Sinha, L.K. & Bhavani, A.G. 2019**.** *Application of GIS and Remote Sensing Technique in Drainage Network Analysis: A Case Study of Naina–Gorma Basin of Rewa District, M.P., India.* P. J. Rao et al. (eds.), Proceedings of International Conference on Remote Sensing for Disaster Management, Springer Series in Geomechanics and Geoengineering.

Smith, M.J. & Clark, C.D. 2005**.** *Methods for the visualization of digital elevation models for landform mapping.* Earth Surf. Process. Landf. 30 (7), 885–900, http: //dx.doi.org/10.1002/esp.1210.

Strahler, A.N. 1964. *Quantitative geomorphology of drainage basins and channel networks. In: Handbook of applied hydrology.* McGraw-Hill, New York, pp 439–476.

Tlapáková, L., Žaloudík, J, Kulhavý, Z. & Pelíšek, I. 2015**.** *Use of Remote Sensing for Identification and Description of Subsurface Drainage System Condition.* Acta Universitatis Agriculturae et Silviculturae Mendelianae Brunensis, 63(5): 1587–1599.

Trudgill, B.D. 2002. *Structural controls on drainage development in the Canyonlands grabens of southeast Utah.* AAPG Bulletin, 86 (6), 1095-1112.

Wołosiewicz, B. 2018. *The influence of the deep seated geological structures on the landscape morphology of the Dunajec River catchment area, Central Carpathians, Poland and Slovakia.* Contemporary Trends in Geoscience, 7(1), 21-47.

Received at: 11. 12. 2021
Revised at: 09. 01. 2022
Accepted for publication at: 02. 02. 2022
Published online at: 05. 02. 2022